

# Compact object coalescence rate estimation from short gamma-ray burst observations

Carlo Enrico Petrillo

*Dipartimento di Scienze Fisiche, Università di Napoli "Federico II",  
Compl. Univ. Monte S. Angelo, Ed. N, Via Cinthia, I-80126 Napoli, Italy*

Alexander Dietz

*Department of Physics and Astronomy, 108 Lewis Hall,  
The University of Mississippi, University, Mississippi 38677-1848*

Recent observational and theoretical work increase the confidence that short-duration gamma-ray bursts are created by the coalescence of compact objects, like neutron stars and/or black holes. From the observation of short-duration gamma-ray bursts with known distances it is possible to infer their rate in the local universe, and draw conclusions for the rate of compact binary coalescences. Although the sample of such events with reliable redshift measurements is very small, we try to model the distribution with a luminosity function and a rate function. The analysis performed with a sample of 15 short gamma-ray bursts yields a range for the merger rate of 75 to 660  $\text{Gpc}^{-3}\text{yr}^{-1}$ , with a median rate of 180  $\text{Gpc}^{-3}\text{yr}^{-1}$ . This result is in general agreement with similar investigations using gamma-ray burst observations. Furthermore, we estimate the number of coincident observations of gravitational wave signals with short gamma-ray bursts in the advanced detector era. Assuming each short gamma-ray burst is created by a double neutron star merger, the expected rate of coincident observations is 0.1 to 1.1 per year, when assuming each short gamma-ray burst is created by a merger of a neutron star and a black hole, this rate becomes 0.4 to 4.0 per year.

## I. INTRODUCTION

Short Gamma-Ray Bursts (SGRB) are some of the most powerful explosions detected in the universe. They are intensive bursts of high energy gamma rays with a duration shorter than two seconds [1], with isotropic energies exceeding  $10^{52}$  ergs. The most common interpretation of their progenitors is a system of two compact objects, either two neutron stars (NS–NS) or a neutron star and a black hole (NS–BH), which undergo a merger [2, 3]. According to General Relativity the orbits of these objects shrink due to emission of gravitational waves, before they coalesce to form a single black hole. Because of the emission of gravitational waves, these objects are one of the primary sources for ground-based gravitational-wave detectors, such as LIGO [4] and Virgo [5]. A detection of a GW signal on its own is already very interesting, as it allows to draw conclusions on the NS equation of state [6, 7], will allow tests of general relativity in the strong-field regime [8], to set limits on the graviton mass [9, 10], and to test the Lorentz Invariance principle [11]. Detection of GW signals in coincidence with optical counterparts, such as a GRB, will not only increase the confidence that the GW signal is real, but also adds much more to the scientific outcomes. If, for example, the redshift  $z$  of the GRB can be measured, it becomes possible to measure cosmological distances *without* the cosmological distance ladder (see e.g. [12] and references therein). Even if e.g. the Hubble parameter can be constrained from GW observations alone [13], coincident detections will help to vastly improve the precision of such measurements [14]. GW-GRB observations will therefore become very important in the future in the area of cosmology.

In this paper we estimate the local merger rate of compact objects, as well as the number of expected GW-SGRB observations in the advanced GW-detector era. Short GRB data with redshifts from SWIFT observations are fitted to a theoretical model. In order to avoid selective bias, only SWIFT GRBs are

used, and each redshift association is carefully examined, rejecting any GRB with an uncertain association. Furthermore, in contrast to a previous study [15], the individual measured luminosities of each GRB are incorporated to improve the result, and a more complete data sample is used.

This paper is organized as follows: Section II describes the available data of SGRB used in this work and the fitting models. Results are discussed in section III and compared to rate estimates from other works or obtained with alternative methods.

## II. DATA AND MODELS

We use the set of SGRB with reliable redshift measurements as listed in [15], complemented by three additional SWIFT SGRBs with reliable redshift measurements [16]. See Appendix A for details on the selection of the additional GRBs. Restricting the analysis to 17 SWIFT GRBs with a reliable redshift measurement, we eliminate any instrumental bias with respect to GRBs detected by other GRB missions.

The (apparent) luminosity of these GRBs is computed using the redshift and fluence information, as given in Table I. To approximate the flux  $F$  in the observer frame, which is the relevant frame for the detection threshold of the satellite, the GRB fluence  $S$  is divided by its duration. As the observed fluence depends on the spectral properties of the source and the energy response of the detector, 15 to 150 keV for the BAT instrument onboard SWIFT [17], and we observe sources over cosmological distances, we expect a spectral shift and a change of fluence for two identical sources at different distances. As the observed photon number spectrum can be well expressed by the Band function [18], it is possible to calculate the spectral shift as a function of redshift (see, e.g., Refs [19, 20]). However, as most sources for the short GRBs are closer than  $z = 1$ , it can be shown that, using the Band function with reasonable

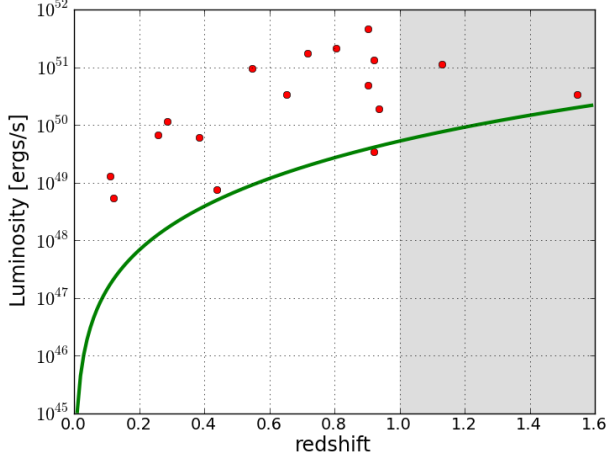


FIG. 1. Distribution of the used SGRB as a function of luminosity and redshift. Only 17 of these 19 SGRBs are used in this paper (unshaded area), with a redshift smaller than 1.

parameters as given, e.g., in Ref. [20], the effect of the spectral shift is less than 10%. As this error is small compared to other statistical and systematical errors, we will neglect the effect of spectral shift in this work. The apparent luminosity is

$$L = 4\pi d_L^2(z) F \simeq 4\pi d_L^2(z) \frac{S}{T_{90}}, \quad (1)$$

where  $d_L(z)$  is the luminosity distance for a given redshift  $z$ ,  $S$  is the measured fluence and  $T_{90}$  is the time over which the burst emits 90% of its total energy. We adopt a standard flat- $\Lambda$  cosmology with  $H_0 = 71 \text{ km s}^{-1}$ ,  $\Omega_M = 0.27$  and  $\Omega_\Lambda = 0.73$ . The approximate luminosity in the source frame is obtained by multiplying by  $(1+z)$ .

Fig. 1 shows the distribution of the observed luminosities as a function of redshift, with the solid line indicating the approximate threshold on the detector's sensitivity:

$$d_{\text{max}}(L) = \sqrt{\frac{L}{4\pi F_{\text{lim}}}}, \quad (2)$$

where we use the flux threshold as of Ref. [20] with  $F_{\text{lim}} = 5 \times 10^{-9} \text{ erg/s/cm}^2$ . Fig. 1 shows a general trend of missing GRBs above a redshift of  $z \sim 1$ ; this is the so-called *redshift desert* [21]. It is mainly attributed to obscuration effects and red-shifted emission lines in the range between  $z \simeq 1.1$  and  $z \simeq 2.2$  [22]. Restricting to GRBs with redshift smaller than 1 leaves 15 data-points for this analysis.

The data are fitted to a luminosity function, and several commonly used luminosity functions were considered (e.g. a power law, the Schechter function etc., see Refs. [15, 24, 25]). Only the lognormal function produced a reliable fit to the data, so we use this function in the remainder of this work. This lognormal luminosity function is

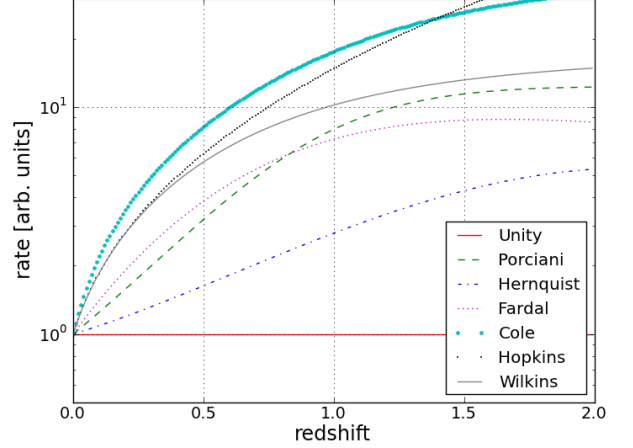


FIG. 2. Comparison of the used rate functions, which are explained in detail in Appendix B. Although we consider only GRBs with redshift 1, the rate function varies significant over this distance range. Not shown in this plot are the delay rate functions.

$$\phi(L) \propto \frac{1}{L} \exp\left(\frac{-(\log L - \log L_0)^2}{2\sigma^2}\right), \quad (3)$$

where  $L_0$  is the mean (peak) value of the luminosity and  $\sigma$  is the width of the distribution. These two parameters are determined by fitting the function to the 15 GRBs in our sample. No evolutionary effects of the luminosity function are taken into account in this work, although some processes might depend on the metallicity of the progenitors [26, 27], which is a function of redshift. Such effects may be included in future work. As this fit only utilizes the *observed* GRBs, we need to rescale the observed luminosity function  $\phi'(L)$  by the volume the satellite is sensitive to, assuming an isotropic distribution of SGRBs:

$$\phi(L) \propto \phi'(L)/d_{\text{max}}^3(L), \quad (4)$$

where  $d_{\text{max}}^3(L)$  is the maximum luminosity distance to which a GRB can be seen (see Eq. (2)).

With the real luminosity function in place, it is now possible to calculate the number of observable SGRB within some redshift distance  $z$ :

$$N'(z) = N_0 \int_0^z dz' \frac{R(z')}{1+z'} \frac{dV(z')}{dz'} \int_{L_{\text{min}}(z')}^\infty \phi(L) dL \quad (5)$$

where  $dV(z')/dz'$  is the comoving volume element and  $N_0$  is a normalization factor. The rate function  $R(z)$  describes the formation rate of binary systems per volume as a function of redshift. Since a binary system of compact objects must be formed from massive progenitor stars,  $R(z)$  can be assumed to follow the star formation rate. Explicit expressions and references for  $R(z)$  used in this work can be found

TABLE I. List of SGRBs with a reliable redshift found by SWIFT between 2004 and 2011. The table includes measured fluences, and redshifts, and the luminosities derived from these quantities as described in the text. The redshift data are taken from [15] or listed in Appendix A, while the fluence data are taken from [23] or taken from the Gamma-Ray burst Coordinated Network, [http://gcn.gsfc.nasa.gov/gcn3\\_archive.html](http://gcn.gsfc.nasa.gov/gcn3_archive.html): <sup>1</sup>GCN6623, <sup>2</sup>GCN7148, <sup>3</sup>GCN7761, <sup>4</sup>GCN8187, <sup>5</sup>GCN9337, <sup>6</sup>GCN10338, <sup>7</sup>GCN11111, <sup>8</sup>GCN11467.

GRB	Duration [s]	Redshift	Fluence [ $10^{-7}$ erg/cm <sup>2</sup> ]
050416	2.0	0.6535	$3.7 \pm 0.4$
050724	3.0	0.2576	$10.0 \pm 1.2$
051016B	4.0	0.9364	$1.7 \pm 0.2$
051221	1.4	0.5465	$11.5 \pm 0.4$
060502B	0.09	0.287	$0.4 \pm 0.1$
060801	0.5	1.131	$0.8 \pm 0.1$
061006	130	0.4377	$14.2 \pm 1.4$
061201	0.8	0.111	$3.3 \pm 0.3$
070429B	0.5	0.9023	$0.6 \pm 0.1$
070714B	64	0.9225	$5.1 \pm 0.3^1$
071227	1.8	0.384	$2.2 \pm 0.3^2$
080520	2.8	1.545	$0.6 \pm 0.1^3$
080905	1.0	0.1218	$1.4 \pm 0.2^4$
090510	0.3	0.903	$3.4 \pm 0.4^5$
100117	0.3	0.92	$0.9 \pm 0.1^6$
100816	2.9	0.8049	$20.0 \pm 1.0^7$
101219	0.6	0.718	$4.6 \pm 0.3^8$

in Appendix B. However, since the time between the formation of the compact objects and the coalescence of the binary are presumably on the order of Gyr [28], a significant delay with respect to the star formation rate can be assumed. This is taken into account by using a delayed rate function in Eq. 5 for two cases (see details in Appendix B). Figure 2 shows the rate functions which differ significantly even over a range of redshifts smaller 1. This indicates, that it is very important to consider various theoretical rate functions in a work like this. Eq. (5) describes the *observable* number of SGRB, so the resulting number  $N'(z)$  need to be divided by a factor  $f_R$ , describing the number of used SGRB to the total number of SGRB during the considered time span (2005 to 2011). During that time span, 49 SGRBs were observed, of which 17 constitute our sample. Therefore  $f_R = 17/49$ , with an estimated error of about 20% ( $\sqrt{17}/49$ ). The approximate time span spanning the range of data is about  $T = 6$  yr. We further neglect any downtime of SWIFT due to technical issues or other constraints, since this can be neglected compared to other sources of errors. Furthermore, SWIFT has a field of view of about 1.4 sr [17], which means only a fraction  $f_{FOV} \simeq 10\%$  of the whole sky can be seen at a given time. Observations have shown that a short GRB could be created by a soft-gamma repeater, which makes up about 15% of all SGRB [24, 29]. We therefore assume that  $\sim 85\%$  of short GRBs are created by the merger of two compact objects, yielding a correction factor of  $f_{SGR} = 0.85$ . SGRs are in general less luminous than ordinary SGRB, so events at larger redshifts might be composed purely out of SGRB. By

using  $f_{SGR} = 0.85$ , we will obtain a conservative limit on the merger rate.

We also implicitly assume that each merger of two compact objects produces a GRB. In order to create a relativistic outflow and therefore a GRB, a torus must be created around the newly formed black hole. Simulation and theoretical analyzes show that the formation of a GRB depends on several parameters such as spin of the black hole, mass ratio or compactness of the neutron star (see, e.g., [3, 30]). Those parameters are hard to generalize, and assuming each merger produces a GRB is a conservative statement regarding the merger rates we are trying to estimate.

SGRB and GRBs are believed to emit their radiation in a collimated cone, whose half-opening angle  $\theta$  defines the fraction of the sky where the burst can be seen. This fraction is given by  $f_b = 1 - \cos \theta$ . The angle  $\theta$  is highly uncertain, especially in the case of SGRB, as it depends on the model and the Lorentz factor of the outflow [31]. In the following, we adopt the value  $1/f_b = 15$  [32], corresponding to a half-opening angle  $\theta \simeq 20^\circ$ .

With all these corrections in place, the total merger rate  $R_{\text{merger}}(z)$  can be written as

$$R_{\text{merger}}(z) = \frac{f_{SGR}}{T f_b f_{FOV} f_R} N(z). \quad (6)$$

The expected rate of SGRB observations  $R_{\text{SGRB}}(z)$  is

$$R_{\text{SGRB}}(z) = \frac{1}{T} N(z). \quad (7)$$

### III. RESULTS AND DISCUSSION

The fit of eq. (3) to the data yield an *observed* peak luminosity of  $4.2 \times 10^{52}$  ergs/s with a width of  $2.26 \times 10^{52}$  ergs/s. The *true* peak luminosity can be found with Eq. (4) yielding  $1.3 \times 10^{47}$  ergs/s.

The results of this analysis are summarized in Table III, which show the approximated local coalescence rates of binary compact objects for the various rate functions. They are found to be between 150 and 330  $\text{Gpc}^{-3}\text{yr}^{-1}$ . With the large systematic errors on the modeling and the assumptions made above, a more realistic range can be obtained if the minimum rate is halved and the maximum rate is doubled, yielding a rate between 75 - 660  $\text{Gpc}^{-3}\text{yr}^{-1}$ . The median rate is 180  $\text{Gpc}^{-3}\text{yr}^{-1}$ . It should be noted that the upper limit on this rate comes from the model with unity rate function, not assuming any evolution on the star formation over cosmological distances. The calculations have also been repeated with delayed rate functions with delay times of 20 Myr and 100 Myr. This resulted in a rate about 50% larger than without the delay, so the upper limit on our rate estimate need to be increased by 50%. Our final estimation for the merger rate in the local universe is thus 75 - 1000  $\text{Gpc}^{-3}\text{yr}^{-1}$ . However, since 15 % of the observed SGRB could be SGRs instead, the real rates could be even larger.

This result strongly depends on the half-opening angle of the SGRB jets. Figure 3 depicts the dependence of the rate on the opening angle  $\theta$ . The smaller the angle, the larger the real number of merger events must be, since we have to be in the outflow cone to detect the SGRB in the first place. Assuming an half-opening angle of  $10^\circ$ , the merger rate could be as high as several thousand  $\text{Mpc}^{-3}\text{yr}^{-1}$ . A more isotropic large half-opening angle of  $60^\circ$  yields a rate below 100  $\text{Mpc}^{-3}\text{yr}^{-1}$ .

We also predict the number of coincident observations of SGRB with gravitational wave counterparts, assuming that a satellite with a field-of-view comparable to the field of view of SWIFT is operating at the time of advanced GW detectors. Using eq. (7) and the expected ranges for advanced LIGO/Virgo [33], one expects 0.1 to 1.1 coincident observations per year, if SGRB are created by a NS-NS merger (with a range of  $\sim 450$  Mpc), and 0.4 to 4.0 coincident observations

TABLE II. Merger rates summarized by neutron star observation and population synthesis computations, taken from [33].  $R_{\text{low}}$  is a pessimistic estimate,  $R_{\text{re}}$  a realistic estimate and  $R_{\text{high}}$  an optimistic estimate. The results from this work are also included, ranging from 75 to 1000  $\text{yr}^{-1}\text{Gpc}^{-3}$ .

source	$R_{\text{low}}$	$R_{\text{re}}$	$R_{\text{high}}$
NS-NS ( $\text{yr}^{-1}\text{Gpc}^{-3}$ )	10	1000	10000
BN-NS ( $\text{yr}^{-1}\text{Gpc}^{-3}$ )	0.6	30	1000
this work ( $\text{yr}^{-1}\text{Gpc}^{-3}$ )	75 (min)	180 (median)	1000 (max)

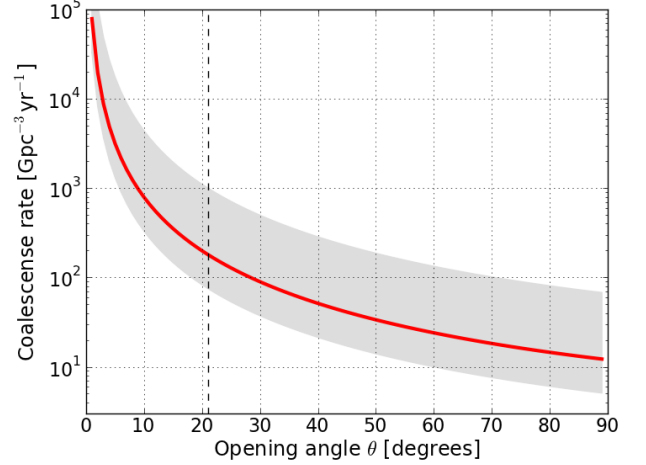


FIG. 3. Coalescence rate of compact objects as a function of the half-opening angle  $\theta$ . The red line indicates the median result while the grey area covers the possible range of rates including the variations from the different fit models and the systematic errors. The vertical, dashed line, indicates the opening angle used for the results in this paper.

per year assuming a NS-BH progenitor (for which the range is  $\sim 930$  Mpc). These values include the systematic uncertainties underlying the estimates, as explained in the previous section. Since the advanced detectors will operate at least some years, these results suggest that it will be unlikely to not observe at least one coincident SGRB-GW event.

If the number of operational GRB satellites changes, these numbers could change significantly. Assuming Fermi in operation during the time of advanced detectors as well as the planned SVOM mission [34] and Lobster[35], the coincident GRB-GW detection rate could be three times as high. Ensuring that at least one GRB mission is operational at the time of advanced detectors will be crucial to gain valuable information, like redshift, host galaxy, the galaxy

TABLE III. Coalescence rates from modeling the observed 15 SGRB, and the estimated detections per year for advanced LIGO/Virgo with a reach of 450 Mpc for NS-NS systems and 930 Mpc for NS-BH systems, respectively.

Rate model	rate $\text{Gpc}^{-3}\text{yr}^{-1}$	NS-NS $\text{yr}^{-1}$	NS-BH $\text{yr}^{-1}$
Unity	333	171	1123
Wilkins	171	64	577
Hopkins	155	58	524
Fardal	179	74	605
Cole	149	52	501
Hernquist	259	125	873
Porciani	156	60	492
Porciani, 20 Myr	252	117	849
Porciani, 100 Myr	259	120	874

star formation rate etc, in addition to the parameters of the gravitational wave. Even if only one GRB mission will be operational, with an observing time of several years, there could be a good chance to get a few observations.

The results obtained in this work can be compared to results obtained elsewhere. Two approaches are usually taken to estimate the rate of merger of compact objects. The first is to infer the rates from observed pulsar observations [36]. The other approach is to employ population synthesis models [37]. Both approaches inherit large statistical or systematical errors. A recent review article [33] summarizes those results, concluding the real rate of merger events is somewhere between 10 and 10000  $\text{Gpc}^{-3}\text{yr}^{-1}$ . Compared to that rate, the estimation in this work is more conservative.

In this approach, the spatial distribution of observed short GRB with known redshift is fitted against a luminosity model and/or a rate function, from which the merger rate can be deduced. Several investigations have been made in the past using this approach. Reference [38], for example, finds a range of  $8\text{-}30\text{Gpc}^{-3}\text{yr}^{-1}$  for SGRBs, although this result is based on 5 samples only. The analysis in [15] yields a much higher rate of about  $7800\text{Gpc}^{-3}\text{yr}^{-1}$  with a sample of 7 (15) SGRB, but this work neglects the individual GRB luminosities. Finally, a recent study uses a different approach focusing on single GRB observations [19]. The maximum distance at which each SGRB could be detectable by SWIFT is calculated, and converted into a final local rate. This study finds a merger rate of 0.2 to  $230\text{Gpc}^{-3}\text{yr}^{-1}$  which overlaps with our rate estimation.

Despite the various approximations used, our value of expected detected mergers by LIGO is broadly consistent with that based on extrapolations from observed binary pulsar in our galaxy and population synthesis model [33]. The method used in our work seems to be one of the most promising, especially with growing statistics of further observations of SGRBs.

## ACKNOWLEDGMENTS

The work reported here is the result a summer student project at the University of Mississippi. CEP and his supervisor, AD, were supported by the National Science Foundation through awards PHY-0757937 and PHY-1067985. The authors also would like to thank Marco Cavaglia for his support, and Jocelyn Read and Emanuele Berti for reading the manuscript and making suggestions regarding this work.

## Appendix A: Detailed redshift discussion

This section lists all short GRBs discovered after 2009 with a redshift measurement. For each GRB, the redshift association is scrutinized. Only cases for which an optical afterglow or an unambiguous host galaxy was found, are considered in this work. The numbers in parenthesis correspond to specific circulars of the Gamma-Ray burst Coordinated Network,

[http://gc.n.gsfc.nasa.gov/gcn3\\_archice.html](http://gc.n.gsfc.nasa.gov/gcn3_archice.html).

**GRB 080905** This short GRB has an optical afterglow and a host galaxy [39], making this redshift association reliable.

**GRB 090426** Although an optical afterglow is detected for this short GRB (GCN9255), spectral features indicate a long-GRB nature of this GRB (GCN9296). For that reason this GRB is not considered in our sample.

**GRB 100117** This short GRB has an optical afterglow and a host galaxy [40], making this redshift association reliable.

**GRB 100724** An optical afterglow has been observed (GCN10971), but its spectral features do not allow a precise discrimination between a short or long GRB (GCN10976). For that reason this GRB is not considered in our sample.

**GRB 100816** This short GRB has an optical afterglow and a host galaxy (GCN11123), making this redshift association reliable.

**GRB 101219** The XRT error circle for this GRB contains only one galaxy, from which a redshift obtained (GCN11518). This redshift association is therefore considered reliable.

## Appendix B: Rate functions

This Appendix describes the rate functions used in Eq. 5 in its explicit forms.  $H(z)$  is defined as

$$H(z) = H_0 \sqrt{(1+z)^3 \Omega_M + \Omega_\Lambda}. \quad (\text{B1})$$

*a. Porciani* This function is actually the SF2 formulation given in Ref. [41]

$$R(z) \propto \frac{\exp 3.4 z}{\exp 3.4 z + 22} \quad (\text{B2})$$

*b. Hernquist*

$$R(z) \propto \frac{\chi^2}{1 + \alpha(\chi - 1)^3 \exp(\beta \chi^{7/4})} \quad (\text{B3})$$

with  $\chi(z) = \left[ \frac{H(z)}{H_0} \right]^{2/3}$ ,  $\alpha = 0.012$  and  $\beta = 0.041$  as taken from Ref. [42].

*c. Fardal*

$$R(z) \propto \frac{a^{-p_2}}{(1 + p_1 a^{-p_2})^{p_3+1}} H(z) \quad (\text{B4})$$

with  $p_1 = 0.075$ ,  $p_2 = 3.7$ ,  $p_3 = 0.84$  and  $a \equiv 1/(1+z)$  as taken from Ref. [43].

d. Cole

$$R(z) \propto \frac{a + bz}{1 + \left(\frac{z}{c}\right)^d} H(z) \quad (\text{B5})$$

with different parameters by different authors, summarized in the Table below.

Ref	a	b	c	d
Cole [44]	0.0166	0.1848	1.9474	2.6316
Hopkins [45]	0.0170	0.13	3.3	5.3
Wilkins [46]	0.014	0.11	1.4	2.2

e. *Delayed functions* Because As the merger rate may not follow directly the star-formation rate, since Since the time between the formation of the compact objects and the coalescence of the binary due to the emission of gravitational waves are presumably on the order of Gyr, a significant delay with respect to the star formation rate can be assumed. Therefore, a delayed rate function is defined:

$$R_t(z) = \int_0^{t_d} dt \frac{1}{1 + z_f} R(z_{\text{ret}}) P(t) \quad (\text{B6})$$

with  $P(t)$  representing the probability distribution of the delay time. Population synthesis models [47, 48] suggest this distribution to be a power law

$$P(t) \propto t^\alpha \quad (\text{B7})$$

with  $\alpha \simeq -1$  for  $t > t_{\text{min}}$ .  $z_{\text{ret}}$  is the retarded redshift, i.e. the redshift at the time the compact objects have formed. If  $T(z)$  is the lookback time at redshift  $z$  then

$$z_{\text{ret}} = T^{-1}(T(z) + t) , \quad (\text{B8})$$

with the lookback time  $T(z)$  defined as (see, e.g., [49])

$$T(z) = T_0 \int_0^{dz'} \frac{dz'}{(1 + z') \sqrt{(\Omega_k(1 + z')^3 + \Omega_k(1 + z')^2 + \Omega_\Lambda)}} . \quad (\text{B9})$$

The expression Eq. (B8) contains an integration and function inversion, which is in general solvable by using numerical integration methods. If constraining to flat cosmological models with  $\Omega_k = 0$ , it is possible to solve the integration and write down an analytic expression for the lookback time. This helps to find an analytic expression for B8 and to reduce computational costs dramatically. The necessary steps are shown in Appendix C.

### Appendix C: Analytic lookback times

To solve Eq. B8, an inverse of the integral Eq. B9 is required. If restricting to flat cosmological models with  $\Omega_k = 0$ , one can substitute

$$v := \Omega_k(1 + z)^3 \quad (\text{C1})$$

so the integral takes the form

$$T(z) = \frac{T_0}{3} \int_{v(0)}^{v(z)} dv' \frac{1}{v' \sqrt{v' + \Omega_\Lambda}} . \quad (\text{C2})$$

This has the generic solution

$$T(z) = \frac{T_0}{3\sqrt{\Omega_\Lambda}} (L(v_0) - L(v_1)) , \quad (\text{C3})$$

with setting

$$L(v) := \ln \left( \frac{\sqrt{v + \Omega_\Lambda} + \sqrt{\Omega_\Lambda}}{\sqrt{v + \Omega_\Lambda} - \sqrt{\Omega_\Lambda}} \right) . \quad (\text{C4})$$

This simple analytic expression can be used to calculate the lookback time for a given redshift, instead of evaluating the full integral. With this solution, it is now possible to derive an analytic inverse function of  $T(z)$ . Solving Eq. (C3) for  $L(v_1)$  yields

$$L(v_1) = L(v_0) - 3\sqrt{\Omega_\Lambda} \frac{T}{T_H} \equiv \ln E(T) . \quad (\text{C5})$$

The value of  $L(v_0)$  neither depends on  $z$  nor  $T$ , but is a mere function of  $\Omega_M$  and  $\Omega_\Lambda$  (see Eqs. (C4) and (C1)). Solving Eq. (C4) for  $z$  finally yields

$$z(T) = \left( \frac{\Omega_\Lambda}{\Omega_M} \right)^{1/3} \left[ \left( \frac{1 + E(T)}{1 - E(T)} \right)^2 - 1 \right]^{1/3} - 1 . \quad (\text{C6})$$

- 
- [1] E. Nakar, Phys. Rept. **442**, 166 (2007), arXiv:astro-ph/0701748
- [2] L. Piro, Nature **437**, 822 (2005)
- [3] L. Rezzolla, B. Giacomazzo, L. Baiotti, J. Granot, C. Kouveliotou, *et al.* (2011), arXiv:1101.4298 [astro-ph.HE]
- [4] J. R. Smith (LIGO Scientific), Class. Quant. Grav. **26**, 114013 (2009), arXiv:0902.0381 [gr-qc]
- [5] F. Acernese *et al.*, Class. Quant. Grav. **25**, 184001 (2008)
- [6] Éanna É. Flanagan and T. Hinderer, Phys. Rev. D **77**, 021502 (2008), <http://link.aps.org/abstract/PRD/v77/e021502>
- [7] J. S. Read, C. Markakis, M. Shibata, K. Uryū, J. D. E. Creighton, and J. L. Friedman, Phys. Rev. D **79**, 124033 (Jun. 2009), arXiv:arXiv:0901.3258
- [8] C. M. Will, Living Rev. Rel. **9**, 3 (2005), arXiv:gr-qc/0510072
- [9] A. Stavridis and C. M. Will, Phys. Rev. D **80**, 044002 (Aug 2009)
- [10] D. Keppel and P. Ajith, Phys. Rev. **D82**, 122001 (2010), arXiv:1004.0284 [gr-qc]
- [11] J. Ellis, N. Mavromatos, D. Nanopoulos, A. Sakharov, and E. Sarkisyan, Astropart. Phys. **25**, 402 (2006), ISSN 0927-6505, <http://www.sciencedirect.com/science/article/B6TJ1-4JXY1RR-1/2/84c3810841cfe896d01a49e5b006ce61>
- [12] S. Nissanke, D. E. Holz, S. A. Hughes, N. Dalal, and J. L. Sievers, Astrophys. J. **725**, 496 (2010), arXiv:0904.1017 [astro-ph.CO]
- [13] W. Del Pozzo (2011), arXiv:1108.1317 [astro-ph.CO]
- [14] N. Dalal, D. E. Holz, S. A. Hughes, and B. Jain, Phys. Rev. D **74**, 063006 (Sep 2006), arXiv:0601275 [astro-ph]
- [15] A. Dietz, Astron. Astrophys. **529**, A97 (2011), arXiv:1011.2059 [astro-ph.HE]
- [16] J. Greiner, <http://www.mpe.mpg.de/~jcg/grbgcn.html>
- [17] S. D. Barthelmy *et al.*, Space Science Reviews **120** (2005), arXiv:astro-ph/0507410
- [18] D. Band, J. Matteson, L. Ford, B. Schaefer, D. Palmer, *et al.*, Astrophys. J. **413**, 281 (1993)
- [19] D. Coward *et al.* (2012), to be published
- [20] C. Xiao-Feng, Y. Yun-Wei, C. K. S., and Z. Xiao-Ping (2011), accepted for publication in MNRAS, arXiv:1101.0866 [astro-ph.HE]
- [21] D. M. Coward, D. Guetta, R. R. Burman, and A. Imerito, Mon. Not. Roy. Astron. Soc. **386**, 111 (2008), arXiv:0711.0242 [astro-ph]
- [22] F. Fiore, D. Guetta, S. Piranomonte, V. D’Elia, and L. A. Antonelli, Astron. Astroph. **470**, 515 (2007), arXiv:0704.2189 [astro-ph], <http://dx.doi.org/10.1051/0004-6361:20077157>
- [23] T. Sakamoto *et al.*, Astrophys. J. Suppl. Ser. **175**, 179 (2008), arXiv:0707.4626 [astro-ph]
- [24] R. Chapman, R. S. Priddey, and N. R. Tanvir (2008), arXiv:0802.0008 [astro-ph]
- [25] D. Guetta and L. Stella, A&A **498**, 329 (2008), arXiv:0811.0684 [astro-ph]
- [26] K. Belczynski, M. Dominik, T. Bulik, R. OShaughnessy, C. Fryer, and D. E. Holz, Astrophys. J. Lett. **715**, L138 (2010), arXiv:1004.0386 [astro-ph.HE], <http://stacks.iop.org/2041-8205/715/i=2/a=L138>
- [27] K. Belczynski, T. Bulik, M. Dominik, and A. Prestwich (2011), arXiv:1106.0397 [astro-ph.HE]
- [28] K. Belczynski *et al.*, Astrophys. J. **648**, 1110 (2006), arXiv:astro-ph/0601458
- [29] E. Nakar, A. Gal-Yam, and D. B. Fox, Astrophys. J. **650**, 281 (2006), arXiv:astro-ph/0511254 [astro-ph]
- [30] F. Pannarale, A. Tonita, and L. Rezzolla (2010), arXiv:1007.4160 [astro-ph.HE]
- [31] A. Panaitescu and P. Kumar, Astrophys. J. **571**, 779, arXiv:astro-ph/0109124
- [32] I. Bartos, C. Finley, and S. Marka (2011), arXiv:1108.3001 [astro-ph.HE]
- [33] LIGO Scientific Collaboration and Virgo Collaboration, Class. Quant. Grav. **27**, 173001 (2010), arXiv:1003.2480 [astro-ph.HE]
- [34] J. Paul, J. Wei, S. Basa, and S.-N. Zhang, Comptes Rendus Physique **12**, 298 (2011), arXiv:1104.0606 [astro-ph.HE]
- [35] Priv. com. Neil Gehrels, 2011
- [36] V. Kalogera *et al.*, Astrophys. J. **601**, L179 (2004), arXiv:astro-ph/0312101
- [37] K. Belczynski, V. Kalogera, F. A. Rasio, R. E. Taam, and T. Bulik, Astrophys. J. **662**, 504 (2007), arXiv:astro-ph/0612032
- [38] D. Guetta and T. Piran, A&A **435**, 421 (2005), <http://dx.doi.org/10.1051/0004-6361:20041702>
- [39] A. Rowlinson *et al.*, Mon. Not. Roy. Astron. Soc. **408**, 383 (2010), arXiv:1006.0487 [astro-ph.HE]
- [40] W. Fong, E. Berger, R. Chornock, N. R. Tanvir, A. J. Levan, A. S. Fruchter, J. F. Graham, A. Cucchiara, and D. B. Fox, Astrophys. J. **730**, 26 (2011), <http://stacks.iop.org/0004-637X/730/i=1/a=26>
- [41] C. Porciani and P. Madau, Astrophys. J. **548**, 522 (2001), arXiv:astro-ph/0008294
- [42] L. Hernquist and V. Springel, Mon. Not. Roy. Astron. Soc. **341**, 1253 (2003), arXiv:astro-ph/0209183
- [43] M. A. Fardal, N. Katz, D. H. Weinberg, and R. Dav’e, Mon. Not. Roy. Astron. Soc. **379**, 985 (2007), arXiv:astro-ph/0604534
- [44] S. Cole *et al.* (The 2dFGRS), Mon. Not. Roy. Astron. Soc. **326**, 255 (2001), arXiv:astro-ph/0012429
- [45] A. M. Hopkins and J. F. Beacom, Astrophys. J. **651**, 142 (2006), arXiv:astro-ph/0601463
- [46] S. M. Wilkins, N. Trentham, and A. M. Hopkins (2008), arXiv:0803.4024 [astro-ph]
- [47] K. Belczynski, V. Kalogera, and T. Bulik, Astrophys. J. **572**, 407 (2001), arXiv:astro-ph/0111452 [astro-ph]
- [48] K. Postnov and L. Yungelson, Living Rev. Rel. **9**, 6 (2005), arXiv:astro-ph/0701059
- [49] D. W. Hogg (1999), arXiv:astro-ph/9905116 [astro-ph]